Original Paper

Thermodynamics of redox equilibria and diffusion of polyvalent ions in a phosphate glass melt

Annegret Matthai, Olaf Claußen, Doris Ehrt and Christian Rüssel

Otto-Schott-Institut für Glaschemie, Friedrich-Schiller-Universität, Jena (Germany)

A phosphate glass melt with the basic composition of $NaPO_3 \cdot 2Sr(PO_3)_2$ doped with various oxides of polyvalent elements (Fe_2O_3, As_2O_3, Sb_2O_3, CuO and SO_4^{2-}) was studied with the aid of square-wave voltammetry. The standard potentials depended linearly on temperature. The standard enthalpy ΔH^0 and the standard entropy ΔS^0 of the attributed redox reactions were calculated from the standard potentials measured. The diffusion coefficients were determined from current densities obtained and fulfilled the Arrhenius' law. Both thermodynamics of the redox equilibria and diffusion coefficients are compared with those measured in soda–lime–silica glasses.

Thermodynamik von Redoxgleichgewichten und Diffusion polyvalenter Ionen in einer Phosphatglasschmelze

Eine Phosphatglasschmelze der Zusammensetzung $NaPO_3 \cdot 2Sr(PO_3)_2$, dotiert mit Oxiden verschiedener polyvalenter Elemente (Fe_2O_3, As_2O_3, Sb_2O_3, CuO und SO_4^{2-}), wurde mit Hilfe der Square-Wave-Voltammetrie untersucht. Die Standardpotentiale hingen linear von der Temperatur ab. Die Standardenthalpie ΔH^0 und die Standardentropie ΔS^0 der zugeordneten Redoxreaktionen wurden aus den gemessenen Standardpotentialen bestimmt. Die Diffusionskoeffizienten wurden aus den Stromdichten berechnet und zeigten Arrhenius-Verhalten. Die Thermodynamik der Redoxgleichgewichte und die Diffusionskoeffizienten werden mit den in Kalk-Natronsilicatgläsern erhaltenen Werten verglichen.

1. Introduction

Various properties such as the transmission of glass melts and final glass products are influenced by polyvalent elements and their oxidation states [1 to 3]. Besides this, the fining behavior of the melt is determined by the type and concentration of oxides of polyvalent elements. The redox behavior of polyvalent elements is usually described as follows:

$$M^{(x+n)+} + \frac{n}{2} O^{2-} \rightleftarrows \frac{n}{4} O_2 + M^{x+} \quad (1)$$

with n = number of electrons transferred, O_2 = physically dissolved oxygen, $M^{(x+n)+}$, M^{x+} = polyvalent element in its oxidized and reduced state, respectively.

The equilibrium constants can be determined by equilibrating the glass melt with a gas atmosphere of a well-defined oxygen fugacity, quenching the sample to room temperature and analyzing the solid glass physically or chemically [4 to 8]. This procedure is fairly time-consuming and generally cannot be applied if more than one polyvalent element is present [9 and 10].

In the past few years, numerous studies concerning the thermodynamic behavior of polyvalent elements in glass melts have been carried out with the aid of electrochemical methods, such as cyclic voltammetry [11 to 13] or square-wave voltammetry. Due to its high resolution and sensitivity, square-wave voltammetry is the method most frequently applied today [13 to 17]. These methods enable the determination of standard potentials [13 to 18] and diffusion coefficients [18] or the total quantity of the polyvalent element present. Up to now, voltammetric measurements have been carried out predominantly in soda–lime–silica melts. Here the thermodynamic behavior of various multivalent elements has been studied and numerous diffusion coefficients have been measured [18].

By contrast, the thermodynamics of multivalent elements in phosphate glass melts has scarcely been investigated with the aid of equilibration methods [8 and 19], and up to now, in the literature electrochemical studies in phosphate glass melts have not been reported. This paper provides a study on thermodynamics and diffusion of some multivalent elements in a phosphate glass melt with the aid of square-wave voltammetry.

2. Theory

The redox reaction according to equation (1) can be described by the equilibrium constant $K(T)$:

$$K(T) = \frac{[M^{x+}]}{[M^{(x+n)+}]} [O_2]^{n/4}. \quad (2)$$

The equilibrium constant $K(T)$ depends on the composition of the glass melt as well as on temperature:

Received December 5, 1996, revised manuscript March 17, 1997.

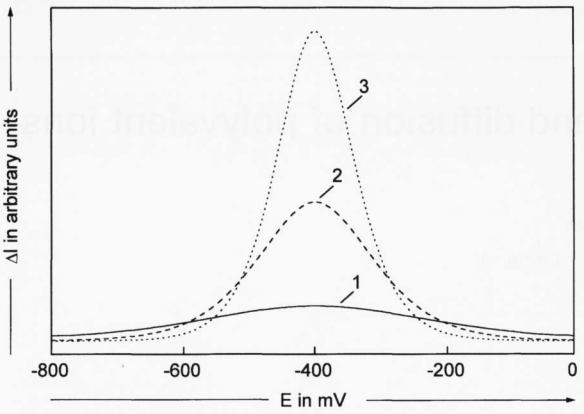

Figure 1. Theoretically calculated current-potential curves for a one-electron step (curve 1), a two-electron step (curve 2) and a three-electron step (curve 3) (ϑ = 1100 °C).

$$\Delta G^0(T) = -R\,T \ln K(T) = \Delta H^0 - T\Delta S^0 \qquad (3)$$

with $\Delta G^0(T)$ = standard free enthalpy, ΔH^0 = standard enthalpy and ΔS^0 = standard entropy.

The standard potential, E_0, can be measured with the aid of voltammetric methods and enables the calculation of both the equilibrium constant $K(T)$ and $\Delta G^0(T)$.

$$\Delta G^0(T) = -n\,F E_0(T)\,. \qquad (4)$$

If the dependence of $E_0(T)$ upon the temperature has been measured, ΔH^0 and ΔS^0 can also be calculated (see equation (3)).

The voltammetric method used was the square-wave voltammetry, its potential-time dependence is a staircase ramp superimposed by a rectangular wave of comparably high frequency (f = 5 to 500 s^{-1}) and amplitude (ΔE^0 = 50 to 250 mV). At the end of every half-wave, the current is measured and then differentiated. The current-potential curves can be calculated using algorithms given in [20 and 21]. Figure 1 shows theoretically calculated current-potential curves for a one, a two and a three-electron step at a temperature of 1100 °C. The half-width of the peak decreases with the number of electrons transferred. The peak currents depend on the surface area of the electrode, A, the total bulk concentration of the polyvalent element, C_0, its self-diffusion coefficient, D, the temperature and on experimental parameters: the pulse time, τ, and the pulse amplitude, ΔE,

$$I_P = 0.31\,\mathrm{A} \cdot C_0 \cdot D^{1/2} \cdot n^2 \cdot F^2 \cdot \Delta E \cdot \tau^{-1/2} \cdot R^{-1} \cdot T^{-1} \cdot \pi^{-1/2}. \qquad (5)$$

With the aid of equation (5), self-diffusion coefficients can be calculated. The temperature dependence of self-diffusion coefficients is given by equation (6):

$$D = D_0\,e^{-E_D/(RT)}. \qquad (6)$$

The peak potentials of the square-wave voltammograms are equal to the standard potentials of the redox couple attributed. For a more detailed description of the theory of square-wave voltammetry see [20 and 21].

3. Experimental

All experiments were carried out in a glass melt with the basic composition $NaPO_3 \cdot 2Sr(PO_3)_2$, modified by adding 0.3 to 1.5 mol% Fe_2O_3, As_2O_3, Sb_2O_3, CuO or $SrSO_4$. The temperatures applied varied in the range of 700 to 1000 °C.

The measurements were carried out in a resistance-heated (SiC) furnace. In the middle of this furnace, a platinum crucible with the glass melt was located. Three electrodes were inserted into this melt: a platinum wire acting as working electrode, a counter electrode consisting of a platinum plate with a size of around 2 cm^2 and a zirconia probe flushed with air as reference electrode. The dip-in length of the working electrode was adjusted to a certain conductivity between working and counter electrode (see [14]).

Potentials mentioned in this paper are referred to the ZrO_2/air electrode. The bulk glass melts need not to be equilibrated with the atmosphere. The vicinity of the working electrode, however, is in equilibrium with that oxygen activity which corresponds to the potential applied (usually 0 mV) before starting the measurement. The electronic equipment was self-constructed: a potentiostat was connected to a microcomputer via analog/digital and digital/analog converter. The potential-time dependence was given by the computer which also recorded the current-potential curve. The experimental procedure is described in detail in [14].

4. Results and discussion

Figure 2a shows a square-wave voltammogram recorded at 900 °C in the phosphate glass melt which was not doped with any polyvalent element. At potentials higher than 0 mV, the current increases due to the formation of oxygen at the platinum electrode. At potentials lower than −700 mV, the current increases drastically caused by the decomposition of the glass matrix. At −580 mV, a slight peak is visible. Applying a pulse amplitude of 100 mV and a pulse time of 10 ms, the peak current is around 2.8 mA. This peak was also observed in phosphate glasses of other compositions, however, it is not to be seen in phosphate-doped silicate glass melts. Phosphate glasses usually contain much higher quantities of water than silicate glasses. From studies of the electric conductivity of phosphate glasses, it is well-known that they are good ionic conductors whose conductivities are exclusively protonic [22 and 23]. This proves that protons or H_3O^+ are highly mobile in these glasses. Other-

wise, they may act as polyvalent ions and give rise to a reduction peak in the voltammogram. The product formed should not be gaseous hydrogen but PH_3, which is thermodynamically favored at these temperatures. Figure 2b shows a current-potential curve of a phosphate glass melt doped with 0.88 mol% Fe_2O_3, recorded at 900 °C. A well-pronounced peak can be observed at a potential of −280 mV. At potentials lower than −720 mV the current increases again. The shoulder at around −630 mV is attributed to the small peak already observed in figure 2b. The peak at −280 mV is attributed to the reduction of Fe^{3+} to Fe^{2+}:

$$Fe^{3+} + e^- \rightleftarrows Fe^{2+}. \quad (7)$$

Figure 3 shows the peak currents as a function of $\tau^{-1/2}$ for the temperatures 900 and 1000 °C. Due to higher diffusion coefficients, the peak currents at 1000 are higher than those at 900 °C. Equation (5) predicts a linear correlation between I_P and $\tau^{-1/2}$. Up to a $\tau^{-1/2}$ value of 0.14 (τ = 50 ms), a nearly linear correlation can be seen. At smaller pulse times, however, a notable deviation from linearity is observed.

Figure 4a shows a square-wave voltammogram of a glass melt doped with 1.48 mol% CuO recorded at 900 °C. A well-pronounced peak possessing a potential of −360 mV is seen. In principle, two redox reactions should be possible. The first is the reduction of Cu^{2+} to Cu^+ and the second the reduction of Cu^+ to metallic copper:

$$Cu^{2+} \overset{e^-}{\rightleftarrows} Cu^+ \overset{e^-}{\rightleftarrows} Cu^0. \quad (8)$$

By comparison, in soda−lime−silica glasses doped with CuO, two distinct peaks are observed which were attributed [15] to both reduction steps in equation (8). From equilibration experiments in phosphate glasses, it is known that if equilibrated with air, copper predominantly occurs in the oxidation state +II [24]. By contrast, in silicate glasses, equilibrated at around 1100 °C with air, the concentrations of Cu^{2+} and Cu^+ are approximately equal. Hence, in equilibration experiments, great differences in the thermodynamics of the Cu^{2+}/Cu^+ equilibrium are observed if silicate glasses are compared with phosphate glasses. Therefore, the peak observed in figure 4a should be caused by the reduction of Cu^{2+} to Cu^+.

In figure 4b, a voltammogram of a glass melt doped with 0.62 mol% As_2O_3 is presented. This voltammogram, also recorded at 900 °C, shows two distinct peaks. The first appears at a potential of −150 mV and is attributed to the reduction of As^{5+} to As^{3+}, while the second peak with a potential of −520 mV corresponds to the reduction of As^{3+} to metallic arsenic:

$$As^{5+} \overset{2e^-}{\rightleftarrows} As^{3+} \overset{3e^-}{\rightleftarrows} As^0. \quad (9)$$

A fairly similar behavior is observed in antimony-doped glass melts. Here, the first peak is observed at a potential

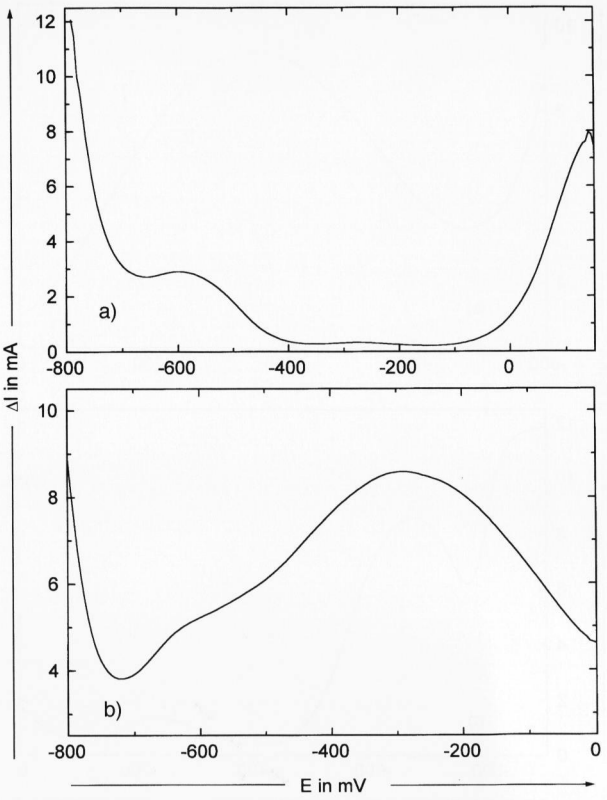

Figures 2a and b. Experimental square-wave voltammogram recorded in a phosphate glass melt (τ = 10 ms, ΔE = 100 mV, ϑ = 900 °C; a) melt without any polyvalent element, b) melt doped with 0.88 mol% Fe_2O_3.

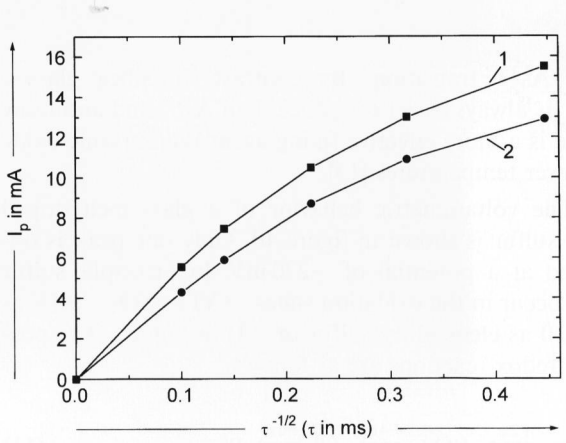

Figure 3. Peak currents of square-wave voltammograms recorded in a phosphate glass melt doped with 0.88 mol% Fe_2O_3 as a function of the pulse time applied. ΔE = 100 mV for curve 1: 1000 °C, curve 2: 950 °C.

of −240 and the second one at −680 mV (see figure 4c). By analogy with arsenic, the electrode reactions are attributed as follows:

$$Sb^{5+} \overset{2e^-}{\rightleftarrows} Sb^{3+} \overset{3e^-}{\rightleftarrows} Sb^0. \quad (10)$$

It should be noted that the peak potential of the Sb^{5+}/Sb^{3+} redox pair is more negative than that of the

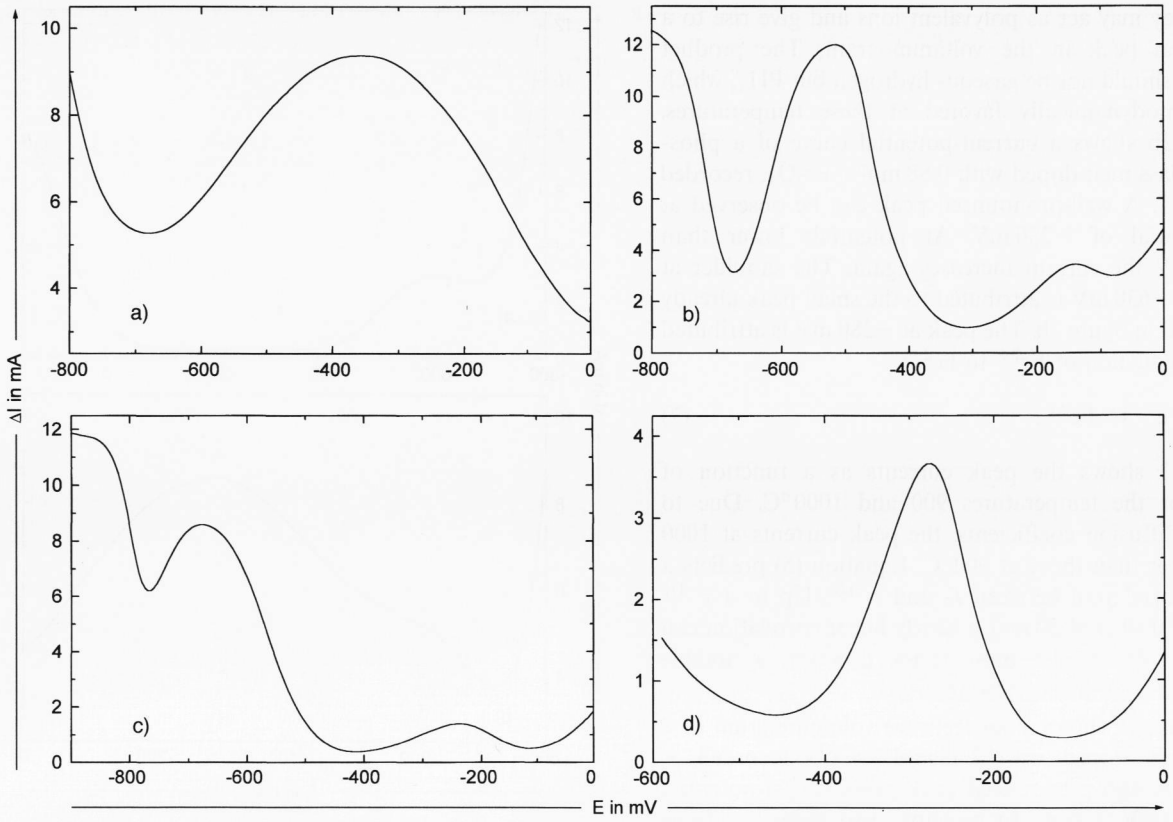

Figures 4a to d. Experimental square-wave voltammograms recorded in a phosphate glass melt (τ = 10 ms, ΔE = 100 mV, ϑ = 900 °C); a) melt doped with 1.48 mol% CuO, b) melt doped with 0.62 mol% As_2O_3, c) melt doped with 0.39 mol% Sb_2O_3, d) melt doped with 0.28 mol% SO_4^{2-}.

As^{5+}/As^{3+} transition. By contrast, in silica glasses, Sb^{5+} is always easier to reduce than As^{5+} and antimony oxide is a more effective fining agent than arsenic oxide at lower temperatures [15].

The voltammetric behavior of a glass melt doped with sulfur is shown in figure 4d. Only one peak is observed at a potential of −270 mV. In principle, sulfur may occur in the oxidation states: +VI as SO_4^{2-}, +IV as SO_2, 0 as elementary sulfur or −II as sulfide. The possible redox reactions are as follows:

$$SO_4^{2-} \underset{-2O^{2-}}{\overset{+2e^-}{\rightleftharpoons}} SO_2 \underset{-2O^{2-}}{\overset{+4e^-}{\rightleftharpoons}} S^0 \overset{+2e^-}{\rightleftharpoons} S^{2-}. \qquad (11)$$

The half-width of the reduction peak is equal to 112 mV. For a two-electron step, a value of 175 mV can be calculated. Thus, the peak in the sulfur-containing glass can be attributed neither to the reduction of sulfate nor to the formation of sulfide. Hence, the conclusion should be drawn that the peak is caused by a four-electron step, the reduction of SO_2 to elemental sulfur. In soda−lime−silica glasses, a peak at comparable potentials, but additionally another one at more negative potentials were observed [17]. The first peak approximately possessed the same half-width as that in figure 4d and has also been attributed to the reduction of physically dissolved SO_2. The second peak which in [17] has been related to the formation of sulfide, is not observed in figure 4d, however. Since the SO_4^{2-}/SO_2 redox step describes the fining reaction of sulfate, its standard potentials at fining temperature possess a positive potential outside the voltammetrically accessible potential range. Extrapolation of the peak potential measured towards 1500 °C, however, still results in negative potentials. Thus, the peak observed cannot be caused by the SO_4^{2-}/SO_2 redox couple.

All voltammograms shown in figures 2b and 4a to d were recorded at 900 °C. The peak potentials measured, however, depend on temperature. At all elements investigated, the peak potentials are shifted towards lower values while decreasing the temperature. This is illustrated in figure 5 for each reduction step observed. In any case linear dependences of the peak potentials upon temperature were observed. Thus, according to equation (3), both standard enthalpies and standard entropies of the redox reactions can be calculated. The obtained values are summarized in table 1, columns 3 and 4. Values of C_{ox}/C_{red}, assuming equilibration with air at 800 °C are summarized in column 5. In column 6, also C_{ox}/C_{red} values calculated from data in soda−lime−silica glasses with the basic composition of $(Na_2O)_{0.16}(CaO)_{0.1}(SiO_2)_{0.74}$ are shown [15].

Table 1. Peak potentials, E_P (at 800 °C), standard enthalpies, ΔH^0, and standard entropies, ΔS^0. The redox ratios were calculated for a temperature of 800 °C assuming equilibration with air for the phosphate glass melt and a soda–lime–silica glass melt $(Na_2O)_{0.16}(CaO)_{0.1}(SiO_2)_{0.74}$.

redox couple	phosphate glass melt				soda–lime–silica glass melt
	E_P in mV	ΔH^0 in kJ mol^{-1}	ΔS^0 in J K^{-1} mol^{-1}	$\lg(C_{ox}/C_{red})$	$\lg(C_{ox}/C_{red})$
As^{5+}/As^{3+}	−170	104	60	1.60	3.65
Sb^{5+}/Sb^{3+}	−273	159	93	2.57	2.82
Fe^{3+}/Fe^{2+}	−325	119	78	1.53	3.07
Cu^{2+}/Cu^{+}	−445	138	85	2.09	–
As^{3+}/As^0	−550	337	153	7.76	8.15
Sb^{3+}/Sb^0	−743	471	229	10.48	5.10

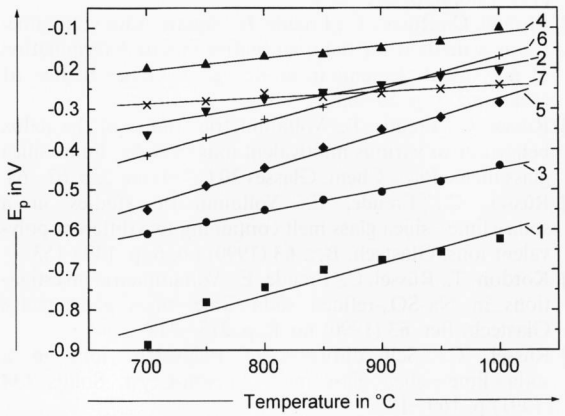

Figure 5. Peak potentials as a function of temperature. Line 1: Sb^{III}/Sb^0, line 2: Sb^{V}/Sb^{III}, line 3: As^{III}/As^0, line 4: As^{V}/As^{III}, line 5: Cu^{II}/Cu^{I}, line 6: Fe^{III}/Fe^{II}, line 7: S^{IV}/S^0.

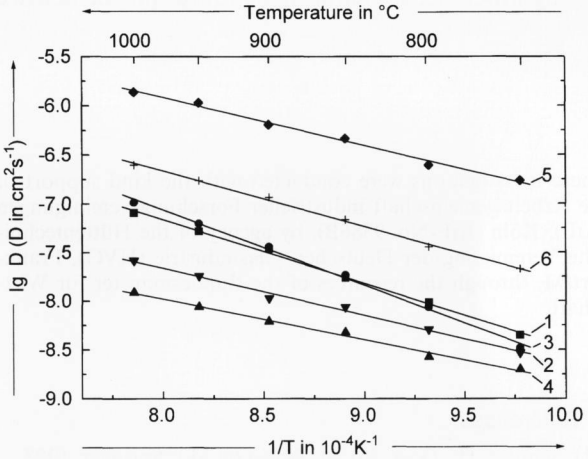

Figure 6. Diffusions coefficients as a function of $1/T$. Line 1: Sb^{III}/Sb^0, line 2: Sb^{V}/Sb^{III}, line 3: As^{III}/As^0, line 4: As^{V}/As^{III}, line 5: Cu^{II}/Cu^{I}, line 6: Fe^{III}/Fe^{II}.

The values of the two glass compositions (see table 1, columns 5 and 6) deviate notably from each other. The electrochemical series of the elements is not at all the same. While the C_{ox}/C_{red} values of the As^{5+}/As^{3+} and Fe^{3+}/Fe^{2+} equilibria are considerably lower in the phosphate glass than in the soda–lime–silica glass melt, that of the Sb^{3+}/Sb^0 equilibrium is much higher. However, the most notable effect is that in phosphate glasses, the As^{5+}/As^{3+} ratio is lower than the Sb^{5+}/Sb^{3+} ratio, while in soda–lime–silica glass melts the opposite effect is observed. Diffusion coefficients of the polyvalent ions were calculated from the attributed peak currents using equation (5). The values are shown in figure 6 as a function of the temperature. The observed linear correlations between $\lg(D)$ and $1/T$ prove that equation (6) is fulfilled and hence, within the temperature range investigated, the activation energies are constant. Diffusion coefficients calculated for a temperature of 800 °C as well as the attributed activation energies are summarized in table 2, columns 2 and 3, respectively. Cu^{2+} possesses the highest diffusion coefficients, while those of As^{5+} and Sb^{5+} exhibit the lowest values. Those of Fe^{3+}, As^{3+} and Sb^{3+} are in between. Generally ions with lower valencies possessed higher diffusion coefficients. This effect was already observed in soda–lime–silica glass melts. Diffusion coefficients of Fe^{3+}, As^{3+} and Sb^{3+} [18] in the soda–lime–silica melt at the same temperature were $1.75 \cdot 10^{-9}$, $1.18 \cdot 10^{-10}$ and $2.21 \cdot 10^{-11}$ cm²/s, respectively. The higher diffusion coefficients in the phosphate melt are supposedly caused by the lower viscosity of this melt.

Table 2. Diffusion coefficients, D (at 800 °C), and activation energies, E_D, for the phosphate glass melt

species	phosphate glass melt	
	D in cm² s^{-1}	E_D in kJ mol^{-1}
As^{5+}	$2.69 \cdot 10^{-9}$	77
Sb^{5+}	$5.13 \cdot 10^{-9}$	92
Fe^{3+}	$3.63 \cdot 10^{-8}$	109
Cu^{2+}	$2.51 \cdot 10^{-7}$	90
As^{3+}	$8.71 \cdot 10^{-9}$	145
Sb^{3+}	$9.77 \cdot 10^{-9}$	122

5. Conclusions

The voltammetrically accessible potential range in the phosphate glass melt investigated is much more narrow

than in silicate melts. This is supposedly due to the reduction of water present in the phosphate melt.

Standard potentials and hence redox ratios of polyvalent elements in phosphate glass melts fairly differ from those in soda–lime–silica glass melts. In the most cases, the C_{ox}/C_{red} ratios were notably lower in the phosphate melt. It is surprising that the redox pair Sb^{5+}/Sb^{3+} possesses lower standard potentials than the As^{5+}/As^{3+} redox pair in the phosphate melt.

The occurring redox states, however, are the same in both melts. The diffusion coefficients calculated from the peak potentials are much higher in the phosphate glass melt than in a soda–lime–silica glass melt previously investigated. By analogy with this silicate melt, ions possessing lower valency show higher diffusion coefficients.

*

These investigations were conducted with the kind support of the Arbeitsgemeinschaft industrieller Forschungsvereinigungen (AiF), Köln (AiF-No. 9386B), by agency of the Hüttentechnische Vereinigung der Deutschen Glasindustrie (HVG), Frankfurt/M, through the resources of the Bundesminister für Wirtschaft.

6. References

[1] Scholze, H.: Glas. 3rd ed. Berlin (et al.): Springer, 1988.
[2] Bamford, C. R.: The application of the ligand field theory to coloured glasses. Phys. Chem. Glasses **3** (1962) no. 6, p. 189–202.
[3] Vogel, W.: Glaschemie. 3rd ed. Berlin (et al.): Springer, 1992.
[4] Paul, A.; Douglas, R. W.: Ferrous–ferric equilibrium in binary alkali silicate glasses. Phys. Chem. Glasses **6** (1965) no. 6, p. 207–211.
[5] Lauer, H. V. jr.; Morris, R. V.: Redox equilibria of multivalent ions in silicate glasses. J. Am. Ceram. Soc. **60** (1977) no. 9–10, p. 443–451.
[6] Paul, A.: Effect of thermal stabilization on redox equilibria and colour of glass. J. Non-Cryst. Solids **71** (1985) p. 269–278.
[7] Jeddeloh, G.: The redox equilibrium in silicate melts. Phys. Chem. Glasses **25** (1984) no. 6, p. 163–164.
[8] Schreiber, H. D.; Kozak, S. J.; Merkel, R. C. et al.: Redox equilibria and kinetics of iron in a borosilicate glass-forming melt. J. Non-Cryst. Solids **84** (1986) p. 186–195.
[9] Rüssel, C.: Redox reactions during cooling of glass melts – A theoretical consideration. Glastech. Ber. **62** (1989) no. 6, p. 199–203.
[10] Gravanis, G.; Rüssel, C.: Redox reactions in Fe_2O_3, As_2O_5 and Mn_2O_3 doped soda–lime–silica glasses during cooling – A high-temperature ESR investigation. Glastech. Ber. **62** (1989) no. 10, p. 345–350.
[11] Takahashi, K.; Miura, Y.: Electrochemical behavior of glass melts. J. Non-Cryst. Solids **95&96**, Pt. 1 (1987) p. 119–130.
[12] Takahashi, K.; Miura, Y.: Electrochemical studies on redox behavior of metallic ions in molten oxide glasses. Glastech. Ber. **56K** (1983) Bd. 2, p. 928–933.
[13] Freude, E.; Rüssel, C.: Voltammetric methods for determining polyvalent ions in glass melts. Glastech. Ber. **60** (1987) no. 6, p. 202–204.
[14] Montel, C.; Rüssel, C.; Freude, E.: Square-wave voltammetry as a method for the quantitative in-situ determination of polyvalent elements in molten glass. Glastech. Ber. **61** (1988) no. 3, p. 59–63.
[15] Rüssel, C.; Freude, E.: Voltammetric studies of the redox behaviour of various multivalent ions in soda–lime–silica glass melts. Phys. Chem. Glasses **30** (1989) no. 2, p. 62–68.
[16] Rüssel, C.; Freude, E.: Voltammetric studies in a soda–lime–silica glass melt containing two different polyvalent ions. Glastech. Ber. **63** (1990) no. 6, p. 149–153.
[17] Kordon, T.; Rüssel, C.; Freude, E.: Voltammetric investigations in Na_2SO_4-refined soda–lime–silica glass melts. Glastech. Ber. **63** (1990) no. 8, p. 213–218.
[18] Rüssel, C.: Self diffusion of polyvalent ions in a soda–lime–silica glass melt. J. Non-Cryst. Solids **134** (1991) p. 169–175.
[19] Majumdar, R.; Lahiri, D.: Equilibrium studies of Fe in alkali phosphate glasses. J. Am. Ceram. Soc. **58** (1975) no. 3–4, p. 99–101.
[20] Osteryoung, J. G.; O'Dea, J. J.: Square-wave voltammetry. In: Bard, A. J. (ed.): Electroanalytical chemistry. Vol. 14. New York, Basel: Dekker, 1986. p. 209–308.
[21] Barker, G. C.: Square-wave polarography and some related techniques. Anal. Chim. Acta **18** (1958) p. 118–131.
[22] Abe, Y.; Hosono, H.; Akita, O. et al.: Protonic conduction in phosphate glasses, J. Electrochem. Soc. **141** (1994) no. 6, p. L64–L65.
[23] Kotama, M.; Nakanishi, K.; Hosono, H. et al.: Evidence of protonic conduction in alkali-free phosphate glasses. J. Electrochem. Soc. **138** (1991) no. 10, p. 2928–2930.
[24] Hirashima, H.; Yoshida, T.; Brückner, R.: Redox equilibria and constitution of polyvalent ions in oxidic melts and glasses. Glastech. Ber. **61** (1988) no. 10, p. 283–292.

0298P001

Address of the authors:

A. Matthai, O. Claußen, D. Ehrt, C. Rüssel
Otto-Schott-Institut für Glaschemie
Friedrich-Schiller-Universität
Fraunhoferstraße 6
D-07743 Jena